Multiple Lateral Length Scales in Phase-Separating Thin-Film Polymer Blends

H. Wang* and R. J. Composto

Department of Materials Science and Engineering and Laboratory for Research on the Structure of Matter, University of Pennsylvania, Philadelphia, Pennsylvania 19104

E. K. Hobbie and C. C. Han

National Institute of Standards and Technology, Gaithersburg, Maryland 20899

Received November 10, 2000. In Final Form: February 20, 2001

The interplay of phase separation, preferential wetting, and capillary instability in thin-film polymer blends is investigated using composition-profiling and surface-imaging techniques. The phase-separating films exhibit a unique morphology with two evolving lateral length scales at both the free film surface and the interface between the wetting and nonwetting layers. The short-wavelength mode shows power-law growth at both the free film surface and the interface, but with a smaller growth exponent at the surface, implying slower kinetics. The long-wavelength mode shows two power-law growth regimes separated by a plateau.

1. Introduction

In addition to being of profound technological importance, thin films composed of both single and multiple macromolecular components offer a unique opportunity to study the effects of geometrical confinement and reduced dimensionality on the kinetics of dewetting[1−4] and phase separation.[5,6] In the classical model of thin-film breakup originally proposed by Vrij[7] and in the generalization of this model to dewetting introduced by Brochard and Daillant,[8] the fluctuation-induced capillary instability that causes a film to break up is completely analogous to the spinodal instability in binary fluid mixtures, where height fluctuations in the former map onto composition fluctuations in the latter. For polymer blend thin films, previous studies have focused on both *lateral* domain structures within the plane of the film[5] and composition fluctuations, or preferential wetting layers, along a direction *normal* to plane of the film (*surface-directed* spinodal waves),[6] but the interplay of these two mechanisms has received only limited attention, both in simulations[9] and experiments.[10]

In previous studies,[10] we have shown that thin-film polymer blends that undergo phase separation and wetting display three distinct stages of evolution: early, intermediate, and late. The early stage is dominated by the formation of a trilayer structure where the wetting layer phase at the free surface and substrate are (nearly) the same. Subsequently, the minority phase in the middle layer coarsens while the wetting layers thin. Finally, capillary fluctuations rupture the middle layer leading to spinodal dewetting and droplet coarsening. In this paper, we present a detailed study of domain evolution kinetics under the scope of that evolution mechanism where the instability of the confinement-induced interference pattern of the surface-directed composition waves leads to a domain pattern with two distinct lateral length scales: a short-wavelength scale associated with lateral phase separation and a long-wavelength one associated with the lateral breakup of surface-directed composition fluctuations. The time evolution of these two disparate modes, evident as two distinct peaks in the nonequilibrium structure factor, suggests that these films exhibit unique phase-separation dynamics as a function of both the thickness of the film and the depth within the film at which the measurement is performed, pointing to the need for a greater theoretical understanding of the effects of surface enrichment and capillary instability on phase separation and spinodal decomposition in thin-film fluid mixtures.

2. Materials and Methods

The blends used in this study are composed of deuterated poly(methyl methacryalte) (dPMMA, $M_w = 90\ 000$ g/mol, $M_w/M_n = 1.06$) and a random copolymer of poly(styrene-*ran*-acrylonitrile) (SAN, $M_w = 124\ 000$ g/mol, $M_w/M_n = 2.24$) with a mass fraction of 33% acrylonitrile.[11] In the bulk, this blend displays lower critical solution temperature behavior with a critical temperature of roughly 160 °C and a critical composition (ϕ_c) of roughly 0.47, where ϕ denotes the volume fraction of dPMMA. Thin films were prepared by spin-casting a 5% mass fraction solution of the critical blend, dissolved in methyl isobutyl ketone, onto a silicon wafer. To ensure consistent substrates, the native silicon oxide layer

* To whom correspondence should be addressed. Current address: NIST, Polymers Division, Gaithersburg, MD. E-mail: hao.wang @nist.gov.

(1) Xie, R.; Karim, A.; Douglas, J. F.; Han, C. C.; Weiss, R. *Phys. Rev. Lett.* **1998**, *81*, 1251.

(2) Reiter, G. *Phys. Rev. Lett*. **1992**, *68*, 75; *Langmuir* **1993**, *9*, 1344; *Macromolecules* **1994**, *27*, 3046.

(3) Muller-Buschbaum, P.; Vanhoorne, P.; Scheumann, V.; Stamm, M. *Europhys. Lett*. **1997**, *40*, 655.

(4) Thiele, U.; Mertig, M.; Pompe, W. *Phys. Rev. Lett*. **1996**, *80*, 2869.

(5) Sung, L.; Karim, A.; Douglas, J. F.; Han, C. C. *Phys. Rev. Lett*. **1996**, *76*, 4368.

(6) Jones, R. A. L.; Norton, L. J.; Kramer, E. J.; Bates, F. S.; Wiltzius, P. *Phys. Rev. Lett*. **1991**, *66*, 1326. Bruder, F.; Brenn, R. *Phys. Rev. Lett.* **1992**, *69*, 624. Steiner, U.; Klein, J.; Fetters, L. J. *Phys. Rev. Lett*. **1994**, *72*, 1498.

(7) Vrij, A. *Discuss. Faraday Soc.* **1996**, *42*, 23.

(8) Brochard, F.; Daillant, J. *Can. J. Phys.* **1990**, *68*, 1084.

(9) Puri, S.; Binder, K. *J. Stat. Phys.* **1994**, *77*, 145. Puri, S.; Binder, K. *Phys. Rev. E* **1994**, *49*, 5359. Frisch, H. L.; Nielaba, P.; Binder, K. *Phys. Rev. E* **1995**, *52*, 2848.

(10) Wang, H.; Composto, R. J. *Europhys. Lett.* **2000**, *50*, 622; *J. Chem. Phys*. **2000**, 113.

(11) The references to commercial equipment or materials do not imply recommendation or endorsement by the National Institute of Standards and Technology.

10.1021/la001570f CCC: $20.00
Published on Web 03/30/2001

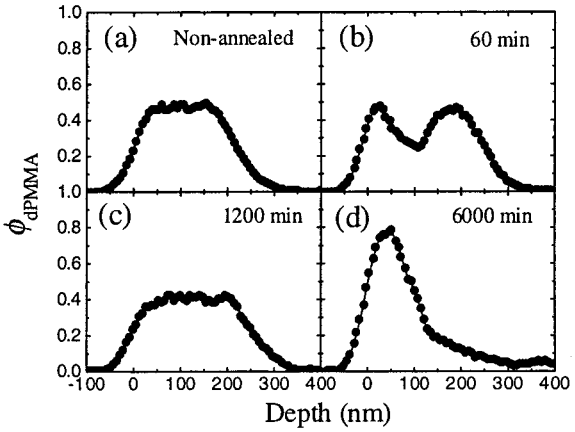

Figure 1. Depth profile of the dPMMA volume fraction, ϕ_{dPMMA}, as measured with FRES for a 223 nm thick film, both in the single phase (a) and at different times following a quench inside the two-phase region (b)−(d).

was removed and a fresh 1.8 nm oxide layer was then reintroduced by exposure to ultraviolet ozone plasma. The films were annealed in a vacuum oven at 120 °C for 24 h, and ellipsometry was then used to measure the film thickness, which varies from 6 to 500 nm.

To study the phase separation as a function of time, the samples were annealed in the two-phase region (185 °C) under argon for times varying from 2 min to 100 h. The dPMMA volume-fraction profile along a direction normal to the plane of the film was measured by forward-recoil spectrometry (FRES), in which 2.00 MeV helium ions impinge on the sample at an angle of +75° with respect to the sample normal. Deuterium and hydrogen from the film are elastically scattered into a solid-state surface barrier detector located at −75° with respect to the sample normal, and an 8 μm Mylar film over the detector prevents forward-scattered He ions from masking the D and H signals of interest. The depth resolution near the surface has a full width at half-maximum value of 50 nm. For the same annealing conditions, the surface roughness and interfacial morphology were measured using a Dimension 3000 atomic force microscope (AFM). To reveal the structure of the nonwetting SAN phase, the dPMMA-rich surface layer was selectively etched away by immersing the film in acetic acid for 2 min. The effect of wet etching has been discussed previously.[10]

3. Results and Discussion

Figure 1 shows the dPMMA volume-fraction profile, measured using FRES, during various stages of phase separation for a 223 nm film, where Figure 1a is the as-cast, homogeneous sample. After 10 min, a dPMMA-rich phase wets both the surface and substrate, but the surface peak is not prominent after convolution with the depth resolution for the measurement. After 60 min (Figure 1b), a dPMMA-rich/SAN-rich/dPMMA-rich trilayer-like structure has developed. After 1200 min (Figure 1c), the sample appears homogeneous, but with a broader composition profile as compared to the as-cast film, suggesting that the film has started to roughen because of a capillary instability of the layers. The area sampled by the incident ion beam is on the order of 3 mm^2, implying that FRES is insensitive to domain structures with wavelengths on the order of 1−10 μm, which is why the sample appears homogeneous in Figure 1c. Finally, after roughly 6000 min (Figure 1d) the free surface becomes wetted by the dPMMA-rich phase, with a thickness of roughly 100 nm, or half the original thickness.

The AFM images reveal in greater detail how the above coarsening proceeds. Figure 2 shows images for different annealing times in the two-phase region of (a) the surface topography and (b) the interfacial morphology after the dPMMA-rich phase has been etched away. In (a), the lighter colored hills correspond to dPMMA-rich regions, and in (b), the lighter colored hills correspond to SAN-rich regions. Note that each image has its own contrast and magnification. Both the surface and interfacial morphologies exhibit two characteristic length scales, a convenient measure of which is obtained from the numerical structure factor calculated from the fast Fourier transform (FFT) of the image. The peak positions are indicated by vertical hatch marks (Figure 2) and evolve toward a lower wave vector (q) with time, reflecting the coarsening of the structures. Because the peaks are superposed on a decaying background, the position of the true maximum appears displaced from the position of the apparent maximum. The wave vectors locating the high- and low-q peaks are $q_h(t)$ and $q_l(t)$, respectively, with the corresponding characteristic length scales $R_h(t) \sim 2\pi/q_h$ and $R_l(t) \sim 2\pi/q_l$. Similar bimodal behavior was observed in both thinner (100 nm) and thicker (500 nm) films, whereas films less than 100 nm exhibit a different evolution mechanism. For films thicker than 1500 nm, surface-directed spinodal decomposition is observed.[12]

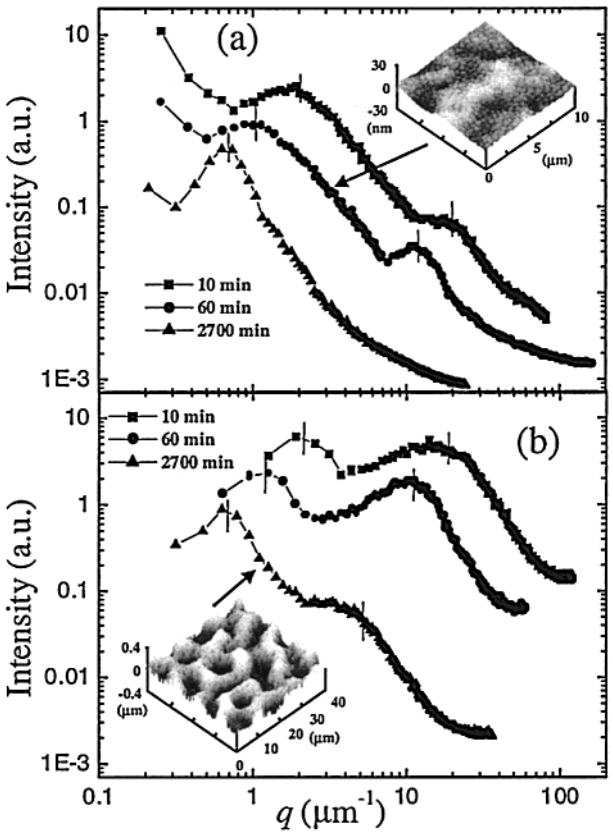

Figure 2. (a) Structure factor calculated from the FFT of the AFM images for different annealing times in the two-phase region for the film shown in Figure 1, where a typical AFM image is shown as an inset. The two peaks correspond to the fine and coarse topography of the free film surface, which is the dPMMA-rich phase. (b) A similar plot as in (a) after the dPMMA-rich phase has been removed. The two peaks correspond to the fine and coarse topography of the underlying SAN-rich structure. The power spectra have a q resolution of 0.15 μm^{-1}.

A detailed description of the physical growth mechanism that dominates during each of the various stages of phase separation is given elsewhere,[10] and here we give a brief qualitative description before quantifying the coarsening kinetics during the time interval 0−6000 min. Initially,

(12) Wang, H.; Composto, R. J. To be published.

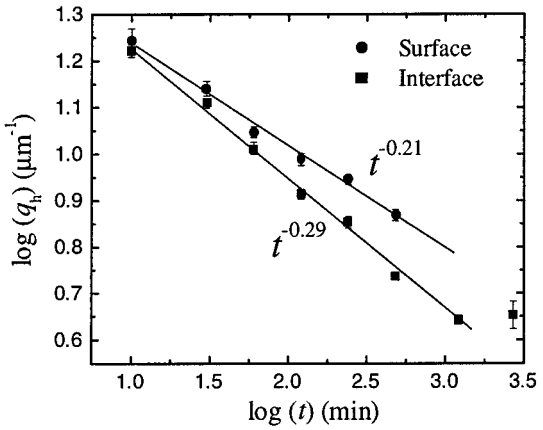

Figure 3. Log−log plot of the time evolution of the position of the high-q peak in Figure 2 for both the surface and interfacial morphologies, where the lines are power-law fits of the data. The interfacial structure evolves with an exponent of around 0.3, whereas the surface structure evolves at a slower rate, with an exponent of around 0.2.

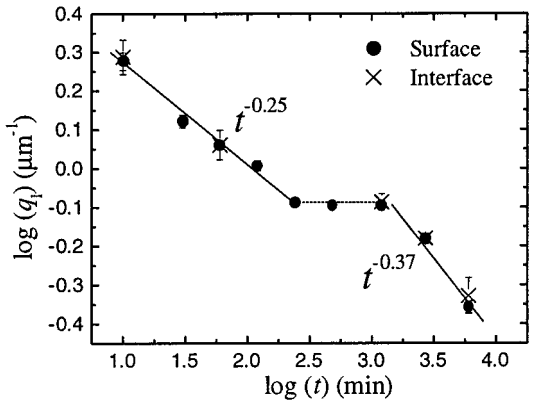

Figure 4. Log−log plot of the time evolution of the position of the low-q peak in Figure 2 for both the surface and interfacial morphologies, where the lines are power-law fits of the data. The surface and interfacial structures have the same time dependence, with a plateau between 240 and 1200 min that corresponds to a pinning of the capillary wavelength while the amplitude continues to increase.

a bicontinuous morphology develops in the bulk of the film, with the wetting component being driven to both surfaces. This leads to the trilayer-like structure with wetting layers of dPMMA-rich phase at both the free film surface and the polymer/silicon oxide interface. A hydrodynamic wetting mechanism causes the surface to roughen. During the intermediate stage, the internal structure coarsens into cylindrical dPMMA-rich domains that bridge the two wetting layers. As these domains coarsen further, the surface layers become thinner and a capillary instability leads to undulations. During the late stage (t > 1200 min), the layers rupture into a bicontinuous morphology, which eventually coarsens into SAN-rich droplets under a dPMMA-rich surface layer. This evolution is a consequence of the undulating free surface. Under hard-wall confinement, such as at the substrate side of the film, the height fluctuations are suppressed, and the surface is flat.

In the above picture, the smaller length scale, $R_h(t)$, corresponds to the "bulk" spinodal wavelength, whereas the longer length scale, $R_l(t)$, corresponds to the wavelength associated with the lateral breakup of nonwetting layers because of thickness undulations, or capillary fluctuations. At the free film surface, a structure of characteristic size R_h appears as small hills (Figure 2a), whereas at the interface between dPMMA-rich and SAN-rich phases, this structure appears as small depressions (Figure 2b). The intensity of the surface peak at q_h reaches a maximum at around 120 min, when the small structures are most prominent, and then starts to decrease. The time dependence of q_h at the surface and interface is shown in Figure 3, which suggests that these fluctuations are initially the same size but then grow in a power-law fashion at different rates, with exponents of 0.21 ± 0.01 at the surface and 0.29 ± 0.01 at the interface. At late times (t ~ 2700 min), the high-q peak at the surface is lost in the shoulder of the low-q peak (Figure 2a).

To our knowledge, such a change in growth kinetics with depth in the film has not been previously reported. Similar behavior is also observed in the 100 nm film, where the exponent varies from 0.14 at the surface to 0.22 at the interface, and the 500 nm film, where the exponent varies from 0.31 at the surface to 0.35 at the interface.[12] Although in the thicker films the interfacial exponents are somewhat close to the value of $^1/_3$ that one might expect in the bulk, we note that the mean lateral dimension of these fluctuations, on the order of 0.5 μm, is greater than or comparable to the mean film thickness, and thus confinement effects should be significant. It seems more likely that the universal dynamic behavior that is so ubiquitous in the bulk,[13] and the unique two-dimensional analogue that has been observed in ultrathin films,[5] is absent here.

Figure 4 shows the time dependence of q_l at the surface and interface, which is insensitive to depth within the film, because the large-scale surface roughness is conformal with interfacial roughness. The size of these fluctuations initially grows in a power-law fashion with an exponent of 0.25 ± 0.02 but then reaches a plateau at 240 min that persists until 1200 min, at which point the growth resumes with an exponent of 0.37 ± 0.08. The plateau corresponds to the regime of time during which the amplitude of undulations increases and the layers ultimately rupture. Both a thinner film (100 nm) and a thicker film (500 nm) show the same behavior, that is, two power-law regimes separated by a plateau, although the data suggest that the growth exponents increase systematically with increasing film thickness.[12] The maximum sizes that the long-wavelength structures achieve at late times are 0.7 μm (6 nm film), 2 μm (45 nm film), 9 μm (100 nm film), 14 μm (223 nm film), and 30 μm (500 nm film), showing a systematic increase with thickness. The late-time domain size for a 20 nm film of the less viscous blend used in ref 5 is 15−20 μm. The exponent of 0.37 ± 0.08 is close to the value reported previously for late-stage dewetting[1] and phase separation.[5]

The obvious difference between the behavior described above and that reported in ref 5 is that here there are two unique lateral length scales associated with two different modes of coarsening. Wetting forces lead to stratification during phase separation, and layers give rise to capillary fluctuations. Recent lattice Boltzmann simulations of phase separation in the presence of surface enriching boundaries illustrate the phenomenon of early-stage layer formation and subsequent late-time capillary instability,[14] and the behavior described here is somewhat reminiscent of that exhibited by bulk polymer blends undergoing spinodal decomposition in the presence of an interfacial wetting force,[15] which show both a "slow" bulklike mode

(13) See, for example: Gunton, J. D.; San Miguel, M.; Sahni, P. S. In *Phase Transitions and Critical Phenomena*; Domb, C., Lebowitz, J. L., Eds.; Academic: London, 1983; Vol. 8.
(14) Martys, N.; Douglas, J. F. *Phys. Rev. E.*, in press.
(15) Wiltzius, P.; Cumming, A. *Phys. Rev. Lett.* **1991**, *66*, 3000. Harrison, C.; Rippard, W.; Cumming, A. *Phys. Rev. E* **1995**, *52*, 723.

($R_S \sim t^{1/3}$) and a "fast" surface-directed mode ($R_F \sim t^b$, where $1.0 < b < 1.5$). Rheologically, the two polymers used in this study are similar,[16] so viscous effects alone probably cannot account for the unusual behavior. Rather, the coupling between capillary fluctuations and coarsening and the surface confinement effect[10] may lie at the foundation of the unusual dynamics, pointing to the need for a deeper theoretical understanding.

4. Conclusions

Using FRES and AFM, the interplay of phase separation, preferential wetting, and capillary instability in thin-film polymer blends has been investigated. The phase-separating films exhibit a unique morphology with two evolving lateral length scales at both the free film surface and the interface between the wetting and nonwetting layers. The physical mechanism of the morphological evolution has been the focus of previous publications.[10] In this article, we report the observation of dissimilar evolution kinetics between short-wavelength surface and interfacial modes, with the surface mode showing the slower growth. In contrast, the long-wavelength surface and interfacial modes exhibit the same kinetics, an early and late-time power-law growth regime separated by a plateau. The depth dependence of the growth kinetics of the short- and long-wavelength modes in phase-separating thin-film polymer blends is discussed, and it is hoped that the experimental evidence presented here might provide more detailed insight into the fundamental nature of nonequilibrium critical dynamics of thin-film binary mixtures.

Acknowledgment. We acknowledge financial support from the NSF DMR program and the NSF MRSEC program and valuable discussions with J. F. Douglas.

LA001570F

(16) Pathak, J. A.; Colby, R. H.; Kamath, S. Y.; Kumar, S. K.; Stadler, R. *Macromolecules* **1998**, *31*, 8988.